Mon. Not. R. Astron. Soc. **000**, 000–000 (0000) Printed 5 February 2008 (MN LATEX style file v2.2)

Radio and X-ray observations of an exceptional radio flare in the extreme z = 4.72 blazar GB B1428+4217

M. A. Worsley,[1] A. C. Fabian[1⋆], G. G. Pooley[2] and C. J. Chandler[3]
[1]*Institute of Astronomy, Madingley Road, Cambridge CB3 0HA*
[2]*Mullard Radio Astronomy Observatory, Cavendish Laboratory, Madingley Road, Cambridge CB3 0HE*
[3]*National Radio Astronomy Observatory, 1003 Lopezville Road, PO Box 0, Socorro, New Mexico 87801, USA*

5 February 2008

ABSTRACT
We report on the extreme behaviour of the high redshift blazar GB B1428+4217 at $z = 4.72$. A continued programme of radio measurements has revealed an exceptional flare in the lightcurve, with the $15.2\,\mathrm{GHz}$ flux density rising by a factor ~ 3 from $\sim 140\,\mathrm{mJy}$ to $\sim 430\,\mathrm{mJy}$ in a rest-frame timescale of only ~ 4 months – much larger than any previous flares observed in this source. In addition to new measurements of the 1.4–$43\,\mathrm{GHz}$ radio spectrum we also present the analysis and results of a target-of-opportunity X-ray observation using *XMM-Newton*, made close to the peak in radio flux. Although the X-ray data do not show a flare in the high energy lightcurve, we are able to confirm the X-ray spectral variability hinted at in previous observations. GB B1428+4217 is one of several high-redshift radio-loud quasars that display a low energy break in the X-ray spectrum, probably due to the presence of excess absorption in the source. X-ray spectral analysis of the latest *XMM-Newton* data is shown to be consistent with the warm absorption scenario which we have hypothesized previously. Warm absorption is also consistent with the observed X-ray spectral variability of the source, in which the spectral changes can be successfully accounted-for with a fixed column density of material in which the ionization state is correlated with hardness of the underlying power-law emission.

Key words: galaxies: active – galaxies: individual: GB B1428+4217 – X-rays: galaxies.

1 INTRODUCTION

Blazars are some of the most extreme extragalactic sources known: powerful, radio-loud active galactic nuclei (AGN) in which the relativistic jet is aligned with the observer's line of sight. Their spectral energy distribution (SED) is dominated by beamed, non-thermal continuum emission from the jet and has a characteristic double-humped shape, with synchrotron radiation from the jet dominating at low energies, and Compton up-scattered emission dominating at high energies. In BL Lac objects (the lower-luminosity class of blazars), the beamed synchrotron emission can peak in the soft X-ray regime, with the second peak dominating the TeV range. For flat-spectrum radio-quasars (FSRQs; the most luminous blazars), the synchrotron radiation tends to peak in the infrared, with the high energy emission peaking in the γ-ray regime (Fossati et al. 1998) and hard ($\Gamma \sim 1.5$) power-law in the X-ray range.

In addition to their extreme luminosity and characteristic SED, blazars often show spectacular broad-band variability, in both absolute brightness and spectral shape. Flares in flux of several tens of per cent have been observed in the radio to TeV regimes in several sources, on timescales of minutes to years depending on wavelength. Blazars show strong, core-dominated and highly-polarised radio emission, strongly supportive of the relativistic jet interpretation. Blazars are usually unresolved although very long baseline interferometry (VLBI) can often reveal superluminal motion on milliarcsecond scales within the nucleus, again consistent with the presence of a relativistic jet.

GB B1428+4217, at a redshift of $z = 4.72$, shows an unexpected flattening of the X-ray power-law continuum at soft X-ray energies. This was first seen in *ROSAT* and *BeppoSAX* observations (Boller et al. 2000; Fabian et al. 2001a) and subsequently confirmed with *XMM-Newton* (Worsley et al. 2004a). A flattening in the X-ray spectral index below observed energies of $\sim 1\,\mathrm{keV}$ has been observed in several other high-redshift, radio-loud sources, e.g.: RBS 315 at $z = 2.69$ (Piconcelli & Guainazzi 2005); PMN J0525−3343 at $z = 4.41$ (Fabian et al. 2001b; Worsley et al. 2004b); RX J1028.6−0844 at $z = 4.28$ (Yuan et al. 2000, 2005a); PMN J1451−1512 at $z = 4.76$ (Yuan et al. 2005b); PKS B1830−211 at $z = 2.51$ (de Rosa et al. 2005); and PKS 2126−0158 at $z = 3.27$ (Fiore et al. 2003; Ferrero & Brinkmann 2003). Although low energy miscalibrations in *ASCA* were initially proposed as an explanation (Grupe et al. 2004), the large number of high-quality

⋆ E-mail: acf@ast.cam.ac.uk

XMM-Newton observations have shown beyond doubt that the effect is real in several objects; that said, a number of *XMM-Newton* observations have also shown that several other high-redshift and radio-loud quasars show no evidence of spectral flattening (Fiore et al. 2003; Grupe et al. 2004, 2006; Piconcelli et al. 2005). A trend toward spectral flattening with increasing redshift has also been seen in several studies of radio-loud objects (e.g. Cappi et al. 1997; Fiore et al. 1998; Reeves & Turner 2000; Bassett et al. 2004).

The origin of the spectral depression is not fully understood, and, whilst the spectral shape of GB B1428+4217 (and other sources) has been repeatedly characterised using an absorbed power-law model, there is not yet sufficient evidence to be certain that intrinsic absorption is the solution. Both Galactic and intergalactic absorption can be effectively discarded as viable solutions given the high column densities required and, critically, by the fact that the phenomenon has not been observed in radio-quiet objects at comparable redshifts (Shemmer et al. 2005; Vignali et al. 2005), which would be expected to be similarly affected by absorption systems lying along the line of sight (O'Flaherty & Jakobsen 1997; Fabian et al. 2001b; Worsley et al. 2004b). The remaining possibilities are absorption intrinsic to the source or an underlying spectral break in the power-law continuum; however, neither explanation can yet be ruled-out in any of the cases of soft X-ray flattening.

As discussed by Fabian et al. (2001b), an underlying break in the continuum could arise in a number of situations. The hard X-ray component of the blazar SED is believed to be due to inverse Compton scattering of seed photons by electrons in the relativistic jet. A spectral break can arise through a low-energy cut-off in the electron population or by a sharply peaked seed photon distribution. Both mechanisms are rather speculative given our limited knowledge of the processes which are important in blazar emission and difficult to reconcile with the sharpness of the X-ray break, which occurs over a range of only a few keV in the rest-frame. An intrinsic absorber, with a column density of $N_{\rm H} \sim 10^{22}$–10^{23} cm^{-2}, remains the most self-consistent explanation for the soft X-ray flattening although very little is known about the nature or origin of the material, which, given the lack of the effect in radio-quiet sources, seems to be closely linked to the presence of jets in these young AGN. X-ray data alone have been unsuccessful in breaking the degeneracy between a cold (neutral) absorber or one that is warm (ionized). In some cases, e.g. for PMN J0525−3343 and RX J1028.6−0844, optical observations have been able to rule-out cold absorption from the lack of a Lyman-limit system at the redshift of the quasar by the presence of emission at rest-frame wavelengths shortward of 912 Å. The lack of such a system in an object means the column density in neutral hydrogen must be $N_{\rm H\,I} \lesssim 3 \times 10^{17}$ cm^{-2}, significantly less than the X-ray implied $N_{\rm H\,I} \sim 10^{22}$–$10^{23}$ cm^{-2}.

In this paper we present the analysis and results from continued radio monitoring of GB B1428+4217, in particular, the details of an exceptional flare in the lightcurve which has seen the 15.2 GHz flux increase by a factor of ~ 3 in only ~ 4 months in the rest-frame of the source. We also report the findings of a recent *XMM-Newton* target-of-opportunity observation performed close to the peak in the radio lightcurve and discuss the X-ray luminosity and spectral evolution displayed by this source. A broad-band radio spectrum is also presented. We adopt $H_0 = 71$ km s^{-1} Mpc^{-1}, $\Omega_{\rm M} = 0.27$ and $\Omega_\Lambda = 0.73$ (Spergel et al. 2003). Errors are quoted at the 1σ (68 per cent) level unless stated otherwise. Also note that any X-ray fluxes quoted are always corrected for Galactic absorption but are not corrected for any intrinsic absorption unless stated otherwise.

2 PREVIOUS OBSERVATIONS

GB B1428+4217 was discovered by Hook & McMahon (1998) as part of survey to identify FSRQs with red optical counterparts (GB B1428+4217 has $R = 20.9$ with $B - R > 3.40$). It is at a redshift of $z = 4.72$, making it one of the most distant X-ray sources known. The blazar has an inverted radio-spectrum, with a 1.4–9 GHz spectral index of $\alpha_{1.4-9} = -0.4$ ($f_\nu \propto \nu^{-\alpha}$). Imaging revealed a core-dominated source with a high level of polarisation (5.5 per cent at 1.5 GHz; Condon et al. 1998). The optical spectrum reveals broad emission lines due to Lyα, N V, the Si IV/O IV] blend and C IV (Hook & McMahon 1998). We will first summarise the findings of previous X-ray and radio observations, before we move on to present the latest results and a joint discussion of the spectrum and variability.

2.1 X-ray spectrum

An X-ray counterpart was found in an archival *ROSAT* Position Sensitive Proportional Counter (PSPC) observation taken in 1992. Subsequent observations were performed with the *ROSAT* High Resolution Imager (HRI; Fabian et al. 1997) and *ASCA* (Fabian et al. 1998). The inferred isotropic X-ray luminosity exceeded 10^{47} erg s^{-1} which suggested highly beamed emission. The 0.5–10 keV data were consistent with a hard power-law spectrum, with a photon index of $\Gamma = 1.29 \pm 0.05$, and an upper limit to any intrinsic absorption at the redshift of the quasar of 4.5×10^{22} cm^{-2} (90 per cent confidence); however, the authors noted that the SIS instrument alone did point to some excess absorption – a column density of $(1.3 \pm 0.6) \times 10^{23}$ cm^{-2} for $\Gamma = 1.43 \pm 0.12$. Excess absorption was confirmed with a further *ROSAT* PSPC observation, which found a power-law index of $\Gamma = 1.4 \pm 0.2$ and a column density of $N_{\rm H}^{\rm cold} = (1.52 \pm 0.28) \times 10^{22}$ cm^{-2} (90 per cent errors) at $z = 4.72$ (Boller et al. 2000). Further observations with *BeppoSAX* also measured $\Gamma = 1.45 \pm 0.10$ power-law and excess absorption of $N_{\rm H}^{\rm cold} = 7.8^{+8.7}_{-6.0} \times 10^{22}$ cm^{-2} (90 per cent errors; Fabian et al. 2001a).

Warm absorption was first suggested by Fabian et al. (2001a) following the *BeppoSAX* observations. In addition to modelling the results of that observation, the authors also fitted the previous *ASCA* and *ROSAT* data. A marginally consistent set of parameters were found with a column density of (2–3) $\times 10^{23}$ cm^{-2} and an ionization parameter $\xi \sim 300$.[1] *XMM-Newton* observations (Worsley et al. 2004a) confirmed the presence of soft X-ray spectral flattening, with a column density of $N_{\rm H}^{\rm cold} \sim (1.4$–$1.6) \times 10^{22}$ cm^{-2} if cold, or up to $N_{\rm H}^{\rm warm} \sim 10^{23}$ cm^{-2} with an ionization parameter $\xi \sim 100$, if due to a warm absorber. Interestingly, the *XMM-Newton* data showed a distinct change in the spectral index of the source, both from the earlier observations as well in the ~ 7 d (rest-frame) between the two *XMM-Newton* exposures. The first observation indicated

[1] Fabian et al. (2001a) quote $\xi_{1-1000\ \rm Ryd}$, defined as $L_{1-1000\ Ryd}/n_{\rm H}R^2$, where $L_{1-1000\ \rm Ryd}$ is the 1–1000 Rydberg luminosity, $n_{\rm H}$ is the space density of H I and R is the distance from the source. For GB B1428+4217, the Fabian et al. (2001a) definition is a factor ~ 2 higher than the $\xi = L_{2-10\ \rm keV}/n_{\rm H}R^2$ definition used in this paper.

$\Gamma \sim 1.9$, whilst the second found $\Gamma \sim 1.75$. Whilst the source had long been known to show extreme luminosity variations, this was the first definitive example of spectral changes.

2.2 X-ray variability

No clear variability was noted between the original *ROSAT* PSPC detection in 1992 and the *ROSAT* HRI and *ASCA* observations during 1996 and 1997: all were consistent with a 0.1–2.4 keV soft X-ray flux[2] of $\sim 10^{-12}\,\mathrm{erg\,cm^{-2}\,s^{-1}}$, with no significant evidence for any differences (Fabian et al. 1997, 1998). However, a series of four *ROSAT* HRI observations from 1997 December 12 until 1998 January 23 showed substantial X-ray variability, with the 0.1–2.4 keV flux increasing from $(0.6 \pm 0.1) \times 10^{-12}$ to $(1.1 \pm 0.1) \times 10^{-12}\,\mathrm{erg\,cm^{-2}\,s^{-1}}$ between the third and fourth exposure – a period of only 2.4 d in the rest-frame of the source (Fabian et al. 1999). Subsequent *ROSAT* PSPC observations then identified 25 per cent variability on a rest-frame timescale of ~ 1.8 h (Boller et al. 2000). Furthermore, the mean 0.1–2.4 keV flux during the observation was $(2.7 \pm 0.6) \times 10^{-12}\,\mathrm{erg\,cm^{-2}\,s^{-1}}$, 3 times the previous *ROSAT* and *ASCA* measurements in this band. A cautionary note must be attached to these PSPC measurements, which were amongst the final observations of the *ROSAT* satellite which experienced some detector anomalies and the development of a large gain hole in the PSPC instrument, although careful data reduction techniques (refer to Boller et al. 2000) should mean the results were not significantly affected. The *BeppoSAX*-measured (Fabian et al. 2001b) 2–10 keV flux and spectral shape imply a 0.1–2.4 keV flux of $\sim 10^{-12}\,\mathrm{erg\,cm^{-2}\,s^{-1}}$, indicating a decrease back to the level seen prior to the *ROSAT* PSPC observation. The two *XMM-Newton* exposures of 2002 December 09 and 2003 January 17 measured 0.1–2 keV fluxes of $(1.17 \pm 0.04) \times 10^{-12}$ and $(0.85 \pm 0.02) \times 10^{-12}\,\mathrm{erg\,cm^{-2}\,s^{-1}}$ respectively, consistent with other measurements but revealing a ~ 30 per cent decrease in the 7 d (rest-frame) between the *XMM-Newton* observations.

In the hard X-ray band, *ASCA* and *BeppoSAX* (Fabian et al. 1998, 2001b) measured consistent 2–10 keV fluxes of 2.5×10^{-12} and $2.76 \times 10^{-12}\,\mathrm{erg\,cm^{-2}\,s^{-1}}$. The two *XMM-Newton* exposures measured 2–10 keV fluxes of $(1.21 \pm 0.06) \times 10^{-12}$ and $(1.08 \pm 0.03) \times 10^{-12}\,\mathrm{erg\,cm^{-2}\,s^{-1}}$ respectively. These were ~ 2–2.5 times lower than the earlier measurements and indicating a 10 per cent decrease in only 7 d (rest-frame) between the *XMM-Newton* observations (note that this decrease is much less than the ~ 30 per cent fall seen for the soft X-ray band because of the distinct change in the spectral shape of the source between the two observations: see Section 2.1). We will present soft and hard band X-ray lightcurves shortly, following the details and results of the new *XMM-Newton* measurements.

2.3 Radio properties

Fabian et al. (1997) collated various radio measurements for GB B1428+4217 and present the SED of the source, noting the flat radio spectrum, high level of polarisation and indications of 5 GHz variability. An intensive monitoring programme was carried out between 1998 April and December using the Ryle Telescope at Cambridge at 15.2 GHz. The programme formed part of a radio and X-ray variability study, although the radio observations were somewhat later than the *ROSAT* HRI exposures carried out in 1997 December and 1998 January (Fabian et al. 1999). The Ryle data revealed significant 15.2 GHz variability, with a flux increase from ~ 100 mJy to ~ 140 mJy in a rest-frame period of only ~ 20 d. The flare ended abruptly mid-way through the observing programme, with the flux decreasing back to ~ 105 mJy within a fraction of a day in the rest-frame. The lightcurve also shows strong variability at the 15 per cent level with a rest-frame timescale of only ~ 2 d.

[2] To reiterate, all X-ray fluxes have been corrected for Galactic absorption only, and not for any apparently intrinsic absorption.

Table 1. VLA measurements of the GB B1428+4217 radio spectrum from 1.425 to 43.4 GHz as measured on 2005 October 14 (MJD 53657), close to the peak in the radio lightcurve. The 15.2 GHz data are from the Ryle Telescope on 2005 October 12. Ryle Telescope flux densities are of Stokes' $I + Q$ but the VLA measurements are of Stokes' I. The flux densities of the calibration source 3C286 are also given.

Frequency (GHz)	GB B1428+4217 flux density (mJy)	3C286 calibrator flux density (Jy)
1.425	171 ± 9	14.70
4.86	273 ± 14	7.47
8.46	348 ± 17	5.20
15.2	380 ± 38	3.50
22.46	367 ± 37	2.52
43.34	290 ± 29	1.45

3 NEW RADIO OBSERVATIONS

The Ryle telescope has been used to measure the 15.2 GHz radio flux of GB B1428+4217 on a regular basis since the monitoring programme in 1997-8 (for details of the observing method see Pooley & Fender 1997). The lightcurve is shown in Fig. 1(a). Measurements after the 1997-8 programme, although sparse, indicated no significant behaviour beyond the variability that had already been observed until that point. The flux decreased to only 70 mJy before starting to climb. In less than 6 months (rest-frame), the flux peaked at ~ 210 mJy before dropping suddenly to 140 mJy. The source then began to steadily grow in flux – the start of a flare of a enormous magnitude that has continued to the present. By 2005 August, the 15.2 GHz flux had reached ~ 430 mJy, a factor ~ 3 increase in only ~ 4 months (rest-frame). The lightcurve continues to show intra-day variations of ~ 10 per cent, with several 'microflares' visible in the primary flare.

A radio spectrum was obtained on 2005 October 14 with the Very Large Array (VLA) at 1.425, 4.86, 8.46, 22.46 and 43.34 GHz, and almost simultaneously at 15.2 GHz with the Ryle Telescope, shortly after the peak flux density at 15.2 GHz (flux densities at this frequency are of Stokes' $I + Q$; all VLA measurements are of Stokes' I). The data and spectrum are given in Table 1 and Fig. 2, respectively. The absolute flux calibration for the VLA data was done using 3C286 and the measured flux densities at each frequency are given in Table 1. The flux measurements include an uncertainty in the calibration of 5 per cent for the three lowest frequencies and 10 per cent for the remainder.

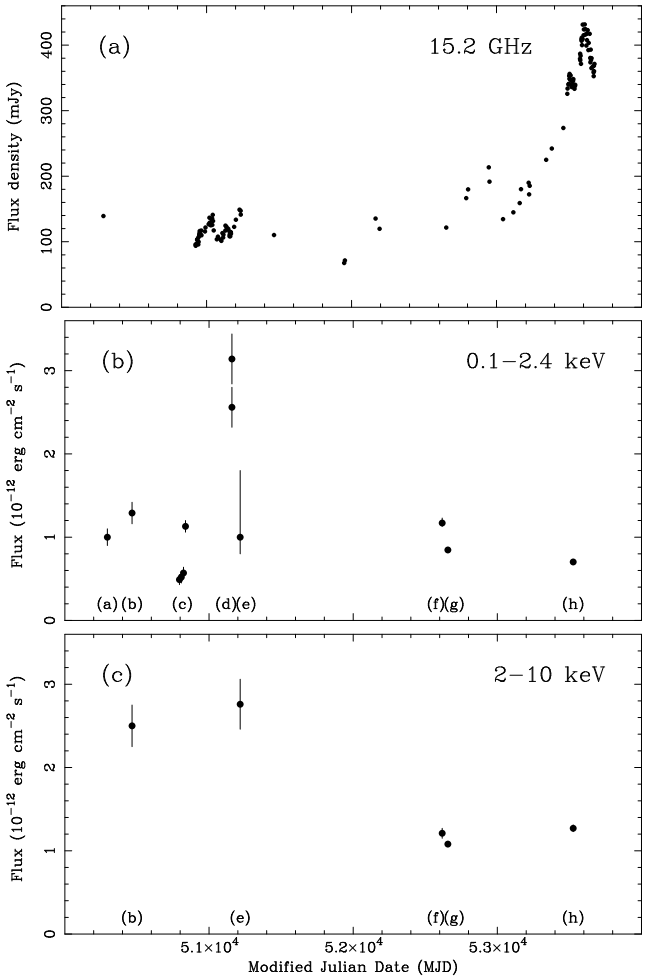

Figure 1. (a) The $15.2\,\mathrm{GHz}$ (rest-frame $86\,\mathrm{GHz}$ radio lightcurve of GB B1428+4217 as measured by the Ryle Telescope in Cambridge from 1998 March 20 (MJD 50923) until 2005 November 01 (MJD 53623). (b) The soft 0.1–$2.4\,\mathrm{keV}$ (rest-frame ~ 0.6–$14\,\mathrm{keV}$) X-ray lightcurve for the same time period. (c) The hard 2–$10\,\mathrm{keV}$ (rest-frame $\sim$ 11–$57\,\mathrm{keV}$) X-ray lightcurve. X-ray Measurements and errors have been taken directly from the reference paper or, where possible, estimated from the spectral parameters and other details. References (in order of observation date): (a) *ROSAT* HRI (Fabian et al. 1997); (b) *ASCA* (Fabian et al. 1998); (c) *ROSAT* HRI (Fabian et al. 1999); (d) *ROSAT* PSPC (Boller et al. 2000); (e) *BeppoSAX* (Fabian et al. 2001a); (f) *XMM-Newton* rev. 549 (Worsley et al. 2004a); (g) *XMM-Newton* rev. 569 (Worsley et al. 2004a); (h) *XMM-Newton* rev. 1005 (this paper).

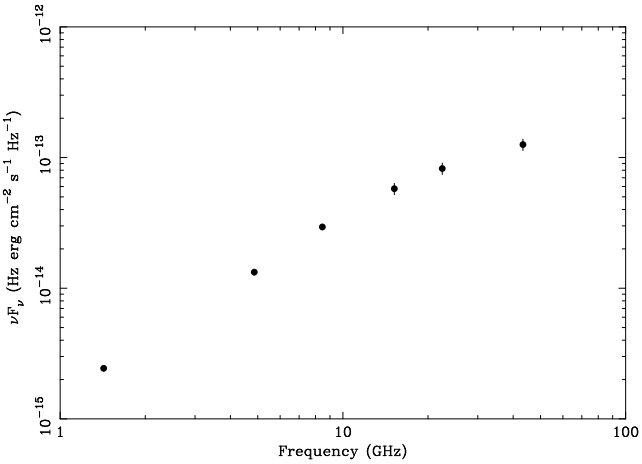

Figure 2. A νF_ν plot showing the radio spectrum of the blazar using data from the VLA and Ryle Telescope. The data are given in Table 1.

4 NEW *XMM-NEWTON* OBSERVATIONS

4.1 Data reduction

Following the extraordinary increase in $15.2\,\mathrm{GHz}$ flux, *XMM-Newton* was used to perform a target-of-opportunity (ToO) X-ray observation co-incident with the radio brightening. Various details of the observation, which was carried out during *XMM-Newton* revolution 1005, are given in Table 2. The European Photon Imaging Camera (EPIC) pn, MOS-1 and MOS-2 instruments were active. Data were reduced using the *XMM-Newton* Science Analysis System (SAS) version 6.4.0-6.5.0. Periods of background flaring were excluded using a lightcurve extracted from the whole pn/MOS chip in each case. Raw events were filtered in the recommended[3] way.

Spectra were produced from events extracted from circular regions centred on the source. Radii of approximately 45 and $75\,\mathrm{arcsec}$ were used for the pn and MOS, respectively. Background spectra were formed using events from nearby source-free regions on the same chip as the source. The regions used had respective radii of approximately 130 and $170\,\mathrm{arcsec}$ for the pn and MOS. The SAS tasks ARFGEN and RMFGEN were used to generate the appropriate response matrices. Background-corrected spectra were produced for each instrument and grouped to a minimum of 20 counts in each energy channel.

4.2 X-ray lightcurve

Figs. 1(b) and 1(c) show X-ray lightcurves to match the radio data shown in Fig. 1(a). Measurements of the X-ray flux in the soft 0.1–$2.4\,\mathrm{keV}$ and hard 2–$10\,\mathrm{keV}$ bands (corresponding to rest-frame energies of ~ 0.6–14 and $\sim$ 11–$57\,\mathrm{keV}$, respectively) are shown. The measurements are taken from the various observations described in Section 2.2 and the new *XMM-Newton* data (2005 June 05). This observation had 0.1–2.4 and 2–$10\,\mathrm{keV}$ fluxes of $(0.70 \pm 0.02) \times 10^{-12}$ and $(1.27 \pm 0.04) \times 10^{-12}\,\mathrm{erg\,cm^{-2}\,s^{-1}}$, respectively. The X-ray lightcurve illustrates the strong variations in flux that have been seen throughout the various observations of the source (see Section 2.2 for details and references). The latest *XMM-Newton* data do not show any evidence of variability within the observation; however, the 0.1–2.4 and 2–$10\,\mathrm{keV}$ fluxes are different to those measured in the previous *XMM-Newton* observations.

There appears to be no obvious correlation between the X-ray and radio lightcurves, although the sparse sampling of the lightcurves does not allow us to rule anything out. Interestingly, one would not necessarily expect a correlation with zero time-lag, particularly since blazar emission is dominated by beamed radiation from a relativistic jet. Continued monitoring in both radio and

[3] `(FLAG==0)&&(PATTERN<=4)&&(PI IN [150,15000])` and `(&XMMEA_EM)&&(PATTERN<=12)&&(PI IN [200,10000])` for the pn and MOS cameras, respectively. See the *XMM-Newton* Science Operations Centre document XMM-SOC-CAL-TN-0018.

Table 2. Details of the ToO *XMM-Newton* observation from revolution 1005 along with the details of the previous exposures of revolutions 549 and 569.

Revolution	Date	MJD	Mode	Filter	Good Exposure Times (ks)			Good counts		
					pn	MOS-1	MOS-2			
549	2002 Dec 09	52617.3	Full frame	Thin	2.6	4.1	4.3	2162	996	979
569	2003 Jan 17	52656.7	Full frame	Thin	11.5	14.2	14.2	6797	2577	2541
1005	2005 Jun 05	53526.3	Full frame	Thin	12.9	15.5	15.9	7222	2604	2657

X-ray wavebands over the coming years may reveal correlations which are not clear with the present data.

4.3 X-ray spectrum

XSPEC version 11.3 was used for spectral fitting, which was done for the pn, MOS-1 and MOS-2 data jointly. A simple power-law model [4], fitted at energies > 1 keV, is a good match to the spectrum, with a reduced chi-squared of $\chi^2_\nu = 1.024$ for $\nu = 316$ degrees of freedom (the probability of the model not representing the data, $1 - \Pr(\mathrm{H}_0)$, is ~ 63 per cent and there is therefore no significant evidence to suggest the model is unacceptable). However, when the same model is applied to the full energy range, the fit is unacceptable (at the 99.998 per cent level), with $\chi^2_{485} = 1.359$. Re-fitting the simple power-law model to the full energy range also leads to an unacceptable fit (at the 99.7 per cent level), with $\chi^2_{483} = 1.187$.

Soft X-ray spectral flattening is once again evident, and we use a power-law plus intrinsic cold absorption model (using ZWABS in XSPEC; Morrison & McCammon 1983). A joint analysis was performed with the earlier *XMM-Newton* data taken in 2002 December and 2003 January (*XMM-Newton* revolutions 549 and 569), respectively; the details are included in Table 2 (for further information on these data refer to Worsley et al. 2004a). Table 3 shows the various results. Allowing the power-law photon index Γ, the ZWABS column density $N_{\mathrm{H}}^{\mathrm{cold}}$, and the normalization to vary between observations can yield good fits to the revolution 549 and 569 data, although the 1005 data is less satisfactory. Fixing Γ and $N_{\mathrm{H}}^{\mathrm{cold}}$ between the observations results in an unacceptable fit (at the 99.994 per cent level), with $\chi^2_{1121} = 1.170$. Alternatively, allowing the $N_{\mathrm{H}}^{\mathrm{cold}}$ to vary whilst Γ is fixed is also unacceptable, with $\chi^2_{1119} = 1.111$ (at the 99.5 per cent level): there is clear spectral variability in the source (a discussion of which we will come to shortly). Interestingly, fixing $N_{\mathrm{H}}^{\mathrm{warm}}$ but allowing Γ to vary leads to a statistically acceptable fit, with $\chi^2_{1119} = 0.999$. All three data-sets are explicable with variations in the underlying power-law slope, with a fixed column density of $(1.4 \pm 0.1) \times 10^{22}$ cm^{-2} of intrinsic cold absorption. This model is not a good fit to the revolution 1005 data on its own ($\chi^2_{484} = 1.095$; unacceptable at the 99.7 per cent level), something which may suggest that the spectrum is more complex, perhaps involving warm rather than cold absorption.

Warm absorption is also a very plausible candidate for the spectral shape of the source. Table 4 shows the results of various power-law plus warm absorption model fits to the data. The photoionization code CLOUDY (Ferland et al. 1998) was used to generate the warm absorber models. The ionization parameter ξ is defined from $\xi = L/n_{\mathrm{H}}R^2$; where L is the rest-frame 2–10 keV luminosity, n_{H} is the absorber space density and R is the distance from the source. As with the cold absorption models we tested various combinations of free and fixed parameters in the analysis. Allowing Γ to vary along with both $N_{\mathrm{H}}^{\mathrm{cold}}$ and the ionization parameter ξ (this is a fixed $\xi = 0$ in the cold absorber models) results in a good fit with $\chi^2_{1114} = 0.985$. Fixing Γ results in a poorer fit with $\chi^2_{1127} = 1.059$, although the evidence for an unacceptable fit is only at the 91.7 per cent level. Allowing Γ and ξ to vary whilst maintaining a fixed $N_{\mathrm{H}}^{\mathrm{warm}}$ provides a very good description of the data, with $\chi^2_{1126} = 0.987$ and reasonable values for the fits to the individual data-sets. A fixed column density of absorption with ionisation state and underlying power-law variations seems the more physically plausible situation and is also consistent with the X-ray spectral variation which we will describe next.

[4] Galactic cold absorption of $N_{\mathrm{H}}^{\mathrm{Gal}} = 1.40 \times 10^{20}$ cm^{-2} (Elvis et al. 1994), applied using WABS in XSPEC (Morrison & McCammon 1983), is included in all spectral models

5 X-RAY SPECTRAL VARIABILITY

The X-ray lightcurves (Figs. 1(a) and 1(b)) show strong amplitude variations but also show differences between the 0.1–2.4 and 2–10 keV behaviour. The $(0.1$–$2.4)/(2$–$10)$ keV flux ratio was ~ 0.5 and then ~ 0.4 during the *ASCA* and *BeppoSAX* observations. The ratio was much larger during the later *XMM-Newton* observations, with more evidence of spectral variation between the revolution 549 and 569 observations, with the ratio falling from 0.97 ± 0.06 to 0.78 ± 0.03. The revolution 1005 data indicate a value of 0.55 ± 0.02, close to that seen in the earlier observations. Here, we have used a simple soft/hard band flux ratio to characterise the spectral variation but the evolution can also be well-described by a change in the underlying power-law slope with a fixed column density of absorption. Fig. 3 shows the X-ray spectra of the three *XMM-Newton* observations and clearly indicates a hardening of the power-law photon index in moving from the revolution 549 to the 569 and 1005 data.

Fig. 4 shows the confidence contours in the power-law slope Γ and the column density $N_{\mathrm{H}}^{\mathrm{cold}}$ of an intrinsic neutral absorber, as measured by the *ROSAT* PSPC, *BeppoSAX*and the three *XMM-Newton* observations. Interestingly, the fixed-$N_{\mathrm{H}}^{\mathrm{cold}}$ but varying-Γ scenario (Table 3(d)), is marginally consistent with all the data-sets. The spectral variations can be explained through variations in the photon index with a fixed absorber column density of $\sim 1.4 \times 10^{22}$ cm^{-2}. These variations, however, do not seem to be correlated with changes in the normalization of the power-law (which is presumably indicated by the 2–10 keV lightcurve in Fig. 1(c)).

The spectral variation can also be explained successfully in the warm absorber scenario. The most self-consistent situation is that of a fixed-$N_{\mathrm{H}}^{\mathrm{warm}}$ but varying-Γ and varying-ξ, i.e. the column density of the absorber remains fixed whilst the ionization state increases with the hardness of the irradiating power-law; indeed, ξ seems to increase with the hardening Γ from revolutions 549, 569 and 1005 (Table 4). This trend can also be visualised in Fig. 5, which shows the X-ray spectrum hardening between the data from *XMM-Newton* revolutions 549, 569 and 1005.

Table 3. Spectral fits to a power-law plus intrinsic cold absorption model (inclusive of Galactic cold absorption of $N_{\rm H}^{\rm Gal} = 1.40 \times 10^{20}$ cm^{-2}). The fits use different combinations of parameters which were fixed to be the same for the separate observations, and those which were free to vary independently. The χ^2_ν and degrees of freedom ν is shown for the total fit and also when the model is applied to the individual data set alone.

Revolution	Γ	$N_{\rm H}^{\rm cold}$ (10^{22} cm^{-2})	Total χ^2_ν	Total ν	Individual χ^2_ν	Individual ν
(a) Γ and $N_{\rm H}^{\rm cold}$ independent:						
549	1.89 ± 0.04	1.61 ± 0.28			0.831	185
569	1.76 ± 0.02	1.67 ± 0.16	0.991	1117	0.946	454
1005	1.49 ± 0.02	0.95 ± 0.15			1.081	484
(b) Γ and $N_{\rm H}^{\rm cold}$ fixed:						
549					1.189	185
569	1.67 ± 0.01	1.40 ± 0.10	1.170	1121	1.005	454
1005					1.308	484
(c) Γ fixed; $N_{\rm H}^{\rm cold}$ independent:						
549		0.51 ± 0.17			1.031	185
569	1.67 ± 0.01	1.15 ± 0.13	1.111	1119	0.989	454
1005		2.12 ± 0.15			1.245	484
(d) Γ independent; $N_{\rm H}^{\rm cold}$ fixed:						
549	1.86 ± 0.27				0.835	185
569	1.73 ± 0.02	1.4 ± 0.1	0.999	1119	0.953	454
1005	1.53 ± 0.02				1.095	484

Table 4. Spectral fits to a power-law plus intrinsic warm absorption model (inclusive of Galactic cold absorption of $N_{\rm H}^{\rm Gal} = 1.40 \times 10^{20}$ cm^{-2}). The fits use different combinations of parameters which were fixed to be the same for the separate observations, and those which were free to vary independently. The χ^2_ν and degrees of freedom ν is shown for the total fit and also when the model is applied to the individual data set alone.

Revolution	Γ	$\log_{10}(N_{\rm H}^{\rm warm}/{\rm cm}^{-2})$	$\log_{10}(\xi/{\rm erg\ cm\ s}^{-1})$	Total χ^2_ν	Total ν	Individual χ^2_ν	Individual ν
(a) Γ, $N_{\rm H}^{\rm warm}$ and ξ independent:							
549	1.89 ± 0.06	22.34 ± 0.21	< -1			0.834	185
569	1.77 ± 0.04	22.37 ± 0.15	-0.04 ± 1.04	0.985	1114	0.945	454
1005	1.55 ± 0.04	22.90 ± 0.67	2.03 ± 0.44			1.061	484
(b) Γ fixed; $N_{\rm H}^{\rm warm}$ and ξ independent:							
549		21.82 ± 0.50	< -1			0.992	185
569	1.70 ± 0.03	22.24 ± 0.13	-0.04 ± 0.96	1.059	1127	0.969	454
1005		> 23	1.84 ± 0.26			1.153	484
(c) Γ and ξ independent; $N_{\rm H}^{\rm warm}$ fixed:							
549	1.91 ± 0.06		-0.96 ± 0.30			0.836	185
569	1.77 ± 0.02	22.34 ± 0.04	-0.18 ± 1.04	0.987	1126	0.946	454
1005	1.51 ± 0.02		1.44 ± 0.15			1.071	484

A fixed $\log_{10}(N_{\rm H}^{\rm warm}/{\rm cm}^{-2}) \sim 22.5$ absorber is consistent with all the data-sets, with the underlying power-law softening from $\Gamma \sim 1.4$ to $\sim$ 1.9, and then hardening back to $\sim$ 1.5 during the *BeppoSAX* and the three *XMM-Newton* observations. A trend is also seen in the ionization parameter, which decreases from $\log_{10}(\xi/{\rm erg\ cm\ s}^{-1}) \sim 1.5$ to ~ 0.8, and then increases to 1.6.

6 CONCLUSIONS

- We have observed an exceptional flare in the 15.2 GHz radio lightcurve of GB B1428+4217. The flux density has grown by a factor of ~ 3 in a rest-frame timescale of only ~ 4 months. The radio lightcurve also shows intra-day variations on the ~ 10 per cent level, consistent with previous observations.
- Target-of-opportunity X-ray observations with *XMM-Newton* do not see any evidence of a flare in the X-ray lightcurve, although the source continues to show $\sim$ 10–25 per cent variability on rest-frame timescales of hours to days.
- The ToO observations are able to confirm the unusual X-ray spectrum of the source, which is well-described by a hard ($\Gamma \sim 1.4$–1.9) power-law with a large amount ($\sim 10^{22}$–10^{23} cm^{-2}) of intrinsic absorption (refer to Worsley et al. 2004a). The present data are unable to discriminate between a cold (neutral) or warm (ionized) absorption (a third possibility, of a spectral break in the power-law continuum, is discussed in detail in our previous paper).
- Previous *XMM-Newton* observations hinted at spectral variations in the source. These have been confirmed with the ToO data, which reveals that the photon index of the X-ray power-law has hardened from $\Gamma \sim 1.7$–1.9, to $\Gamma \sim 1.5$. Interestingly, there is no clear evidence for a change in the column density of the absorption

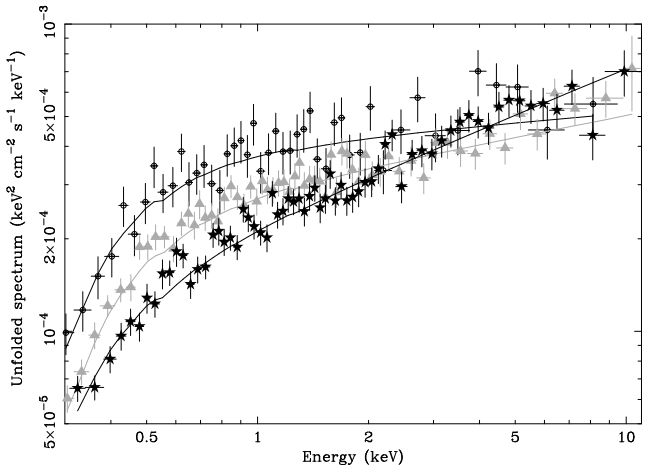

Figure 3. Unfolded X-ray spectra, in νF_ν space, from the *XMM-Newton* revolution 549 (open black circles), 569 (solid grey diamonds) and 1005 (solid black stars) observations. A power-law plus intrinsic cold absorption model was used to unfold the spectra and is shown as a solid line in each case.

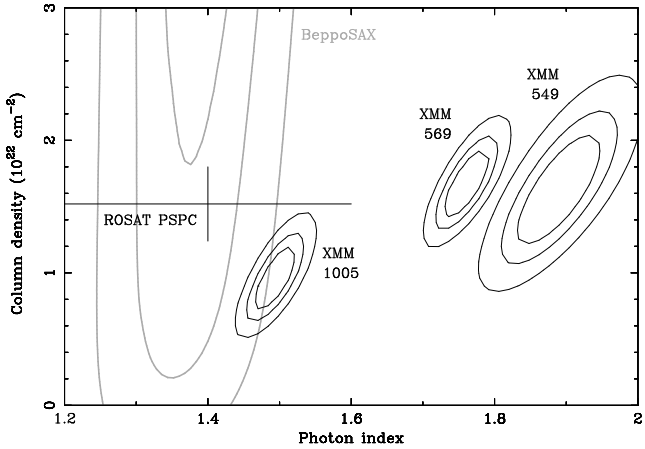

Figure 4. Confidence contours (68, 90 and 99 per cent) in the photon index Γ and the cold absorber column density $N_{\rm H}^{\rm cold}$. The *BeppoSAX* and *ROSAT* PSPC data (Fabian et al. 2001a; Boller et al. 2000) are shown, along with results from *XMM-Newton* revolutions 549, 569 and 1005 (Worsley et al. 2004a; this paper). The data are all marginally consistent with a constant $N_{\rm H}^{\rm cold}$ model in which Γ varies widely, although the column densities implied by the revolution 569 and 1005 data disagree at the 90 per cent level.

in either the cold or ionized absorber scenario. The spectral variations, including all previous data from other telescopes, are consistent with a scenario in which the column density of an ionized absorber remains fixed whilst the ionization state increases with the hardening of the power-law emission.

7 ACKNOWLEDGMENTS

Based on observations with *XMM-Newton*, an ESA science mission with instruments and contributions directly funded by ESA Member States and the USA (NASA). MAW acknowledges support from PPARC. ACF thanks the Royal Society for support. The National Radio Astronomy Observatory is a facility of the National Science Foundation operated under cooperative agreement by Associated Universities, Inc. The authors would also like to thank the referee for helpful comments and suggestions.

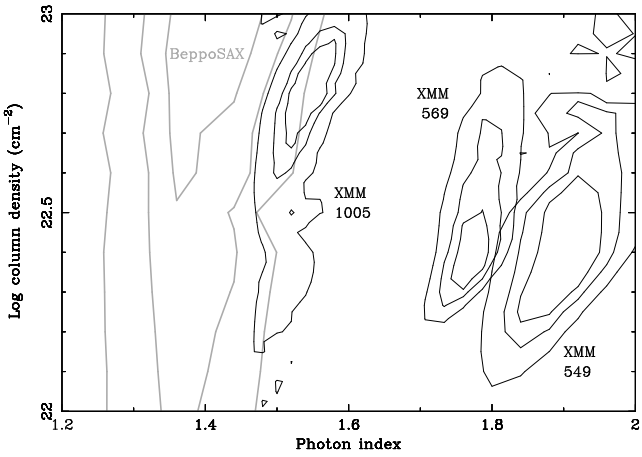

Figure 5. Confidence contours (68, 90 and 99 per cent) in the photon index Γ and the warm absorber column density $N_{\rm H}^{\rm warm}$. Contours are also shown for the *BeppoSAX* data (Fabian et al. 2001a) and the data from *XMM-Newton* revolutions 549, 569 and 1005 (Worsley et al. 2004a; this paper). A fixed-$N_{\rm H}^{\rm warm}$ warm absorber can account for all four observations through strong variations in the power-law slope and ionization parameter.

REFERENCES

Bassett L. C., Brandt W. N., Schneider D. P., Vignali C., Chartas G., Garmire G. P., 2004, AJ, 128, 523
Boller T., Fabian A. C., Brandt W. N., Freyberg M. J., 2000, MNRAS, 315, L23
Cappi M., Matsuoka M., Comastri A., Brinkmann W., Elvis M., Palumbo G. G. C., Vignali C., 1997, ApJ, 478, 492
Condon J. J., Cotton W. D., Greisen E. W., Yin Q. F., Perley R. A., Taylor G. B., Broderick J. J., 1998, AJ, 115, 1693
de Rosa A. et al., 2005, A&A, 438, 121
Elvis M., Lockman F. J., Fassnacht C., 1994, ApJS, 95, 413
Fabian A. C., Brandt W. N., McMahon R. G., Hook I. M., 1997, MNRAS, 291, L5
Fabian A. C., Celotti A., Iwasawa K., Ghisellini G., 2001a, MNRAS, 324, 628
Fabian A. C., Celotti A., Iwasawa K., McMahon R. G., Carilli C. L., Brandt W. N., Ghisellini G., Hook I. M., 2001b, MNRAS, 323, 373
Fabian A. C., Celotti A., Pooley G., Iwasawa K., Brandt W. N., McMahon R. G., Hoenig M. D., 1999, MNRAS, 308, L6
Fabian A. C., Iwasawa K., McMahon R. G., Celotti A., Brandt W. N., Hook M., 1998, MNRAS, 295, L25
Ferland G. J., Korista K. T., Verner D. A., Ferguson J. W., Kingdon J. B., Verner E. M., 1998, PASP, 110, 761
Ferrero E., Brinkmann W., 2003, A&A, 402, 465
Fiore F., Elvis M., Giommi P., Padovani P., 1998, ApJ, 492, 79
Fiore F., Elvis M., Maiolino R., Nicastro F., Siemiginowska A., Stratta G., D'Elia V., 2003, A&A, 409, 57
Fossati G., Maraschi L., Celotti A., Comastri A., Ghisellini G., 1998, MNRAS, 299, 433
Grupe D., Mathur S., Wilkes B., Elvis M., 2004, AJ, 127, 1
Grupe D., Mathur S., Wilkes B., Osmer P., 2006, AJ, 131, 55
Hook I. M., McMahon R. G., 1998, MNRAS, 294, L7
Morrison R., McCammon D., 1983, ApJ, 270, 119

O'Flaherty K. S., Jakobsen P., 1997, ApJ, 479, 673
Piconcelli E., Guainazzi M., 2005, A&A, 442, L53
Piconcelli E., Guainazzi M., Cappi M., Jimenez-Bailon E., Schartel N., 2005, A&A, 432, 835
Pooley G. G., Fender R. P., 1997, MNRAS, 292, 925
Reeves J. N., Turner M. J. L., 2000, MNRAS, 316, 234
Shemmer O., Brandt W. N., Vignali C., Schneider D. P., Fan X., Richards G. T., Strauss M. A., 2005, ApJ, 630, 729
Spergel D. N. et al., 2003, ApJS, 148, 175
Vignali C., Brandt W. N., Schneider D. P., Kaspi S., 2005, AJ, 129, 2519
Worsley M. A., Fabian A. C., Celotti A., Iwasawa K., 2004a, MNRAS, 350, L67
Worsley M. A., Fabian A. C., Turner A. K., Celotti A., Iwasawa K., 2004b, MNRAS, 350, 207
Yuan W., Fabian A. C., Celotti A., McMahon R. G., Matsuoka M., 2005a, MNRAS, 358, 432
Yuan W., Fabian A. C., Worsley M. A., McMahon R. G., 2005b, MNRAS, submitted
Yuan W., Matsuoka M., Wang T., Ueno S., Kubo H., Mihara T., 2000, ApJ, 545, 625